nature physics

Article https://doi.org/10.1038/s41567-022-01816-4

Spin–orbital liquid state and liquid–gas metamagnetic transition on a pyrochlore lattice

In the format provided by the authors and unedited

Supplementary Information for Theoretical Methods

Nan Tang[1,2†], Yulia Gritsenko[3,4†], Kenta Kimura[2,5†], Subhro Bhattacharjee[6], Akito Sakai[1,2], Mingxuan Fu[1,2], Hikaru Takeda[2], Huiyuan Man[2,7], Kento Sugawara[8,9], Yosuke Matsumoto[2,10], Yasuyuki Shimura[2,11], Jiajia Wen[7,12], Collin Broholm[7], Hiroshi Sawa[8], Masashi Takigawa[2,13,14], Toshiro Sakakibara[2], Sergei Zherlitsyn[4], Joachim Wosnitza[3,4], Roderich Moessner[15], Satoru Nakatsuji[1,2,7,16,17*]

[1]*Department of Physics, University of Tokyo, Tokyo 113-0033, Japan*

[2]*Institute for Solid State Physics (ISSP), University of Tokyo, Kashiwa, Chiba 277-8581, Japan*

[3]*Institut für Festkörper- und Materialphysik, Technische Universität Dresden, 01062 Dresden, Germany*

[4]*Hochfeld-Magnetlabor Dresden and Würzburg-Dresden Cluster of Excellence ct.qmat, Helmholtz-Zentrum Dresden-Rossendorf, 01328 Dresden, Germany*

[5]*Department of Advanced Materials Science, University of Tokyo, Kashiwa, Chiba 277-8561, Japan*

[6]*International Centre for Theoretical Sciences, Tata Institute of Fundamental Research, Bengaluru 560089, India*

[7]*Institute for Quantum Matter and Department of Physics and Astronomy, Johns Hopkins University, Baltimore, MD 21218, USA*

[8]*Department of Applied Physics, Nagoya University, Nagoya 464-8603, Japan*

[9]*Synchrotron Radiation Research Center, National Institutes for Quantum Science and Technology, Hyogo 679-5148, Japan*

[10]*Max Planck Institute for Solid State Research, Stuttgart 70569, Germany*

[11]*Department of Quantum Matter, Hiroshima University, Hiroshima 739-8530, Japan*

[12]Stanford Institute for Materials and Energy Sciences, SLAC National Accelerator Laboratory, CA 94025, USA

[13]Toyota Physical and Chemical Research Institute, Aichi 480-1191, Japan

[14]KEK, Institute of Materials Structure Research, Ibaragi 305-0801, Japan

[15]Max-Planck-Institut für Physik komplexer Systeme, 01187 Dresden, Germany

[16]Trans-scale Quantum Science Institute, University of Tokyo, Tokyo 113-0033, Japan

[17]Canadian Institute for Advanced Research, Toronto, ON M5G 1M1, Canada

[†]These authors contributed equally to this work.

1. Microscopics of non-Kramers magnetism

Local basis of a non-Kramers doublet: The Pr^{3+} ($4f^2$ and $J_T = 4$) ions are located in the $D_{3\text{d}}$ crystal field with an axis parallel to the local [111] direction, resulting in a low energy non-Kramers doublet $|\pm\rangle$ that is well isolated from the first excited state by a CEF gap of $\sim$ 10 meV [1,2]. In the local basis, the doublet is given by $\mathrm{s}_i = s_i^x \hat{x}_i + s_i^y \hat{y}_i + s_i^z \hat{z}_i$, where ${s_i}^x$, ${s_i}^y$, ${s_i}^z$ are the pseudospin component along $\hat{x}_i, \hat{y}_i$ and $\hat{z}_i$. The non-Kramers doublet transform under time-reversal operation as

$$\{s_i^x, s_i^y, s_i^z\} \rightarrow \{s_i^x, s_i^y, -s_i^z\}. \tag{1}$$

The longitudinal (transverse) spin component(s), s_i^z (s_i^x, s_i^y) arise from the projection of dipole (quadrupole) operators of the underlying $\mathbf{J}$ moments to the ground-state doublet.

Spin Hamiltonian: The symmetry allowed nearest neighbour spin Hamiltonian is given by[3]

$$H_s = \sum_{\langle ij \rangle} \left[J_{zz} s_i^z s_j^z + J_{\pm}(s_i^+ s_j^- + s_i^- s_j^+) + J_{\pm\pm}(\gamma_{ij} s_i^+ s_j^+ + \gamma_{ij}^* s_i^- s_j^-) \right], \tag{2}$$

where J_{zz} and $J_{\pm}$ are Ising and XY-like spin couplings, respectively. The $J_{\pm\pm}$ term comprises a bond-dependent phase factor $\gamma_{ij} = 1, \omega, \omega^2$ that cannot be gauged away except for an overall sign.

Coupling of the pseudospins with the lattice vibrations: To capture the physics of spin-phonon coupling in $Pr_2Zr_2O_7$, we introduce the elastic modes of a single tetrahedron– the basic unit of the pyrochlore lattice. The six vibration modes of the tetrahedral group are: singlet (ε_A), doublet ($\boldsymbol{\varepsilon}_E \equiv (\varepsilon_E^{(1)}, \varepsilon_E^{(2)})$) and triplet ($\boldsymbol{\varepsilon}_T \equiv (\varepsilon_T^{(1)}, \varepsilon_T^{(2)}, \varepsilon_T^{(3)})$).

A non-Kramers system features primarily two types of spin-lattice couplings– (a) linear, and, (2) quadratic in the pseudospins. To derive the form of these couplings for a single tetrahedron level, we use the irreducible representations of the tetrahedral group, T_d, as well as time reversal symmetry given in Table 1.

Therefore the spin-lattice coupling Hamiltonian is given by

$$H_{\mathrm{S-L}} = H^{Q}_{\mathrm{sl}} + H^{sl}_{M} + \tilde{H}^{Q}_{sl}. \tag{3}$$

<u>*Linear magneto-elastic coupling:*</u> The linear coupling between the transverse component of the pseudospins and the lattice vibration is given by

$$H^{Q}_{\mathrm{sl}} = \sum_{\boxtimes} \left(\lambda_E\, \boldsymbol{\varepsilon}_E \cdot \mathbf{Q}_E + \lambda_T \boldsymbol{\varepsilon}_T \cdot \mathbf{Q}_T\right), \tag{4}$$

where $\mathbf{Q}_E$ and $\mathbf{Q}_T$ are the corresponding quadrupole modes of the tetrahedron. This term is unique to the non-Kramers systems.

<u>*Quadratic magneto-elastic coupling:*</u> The conventional magneto-elastic couplings are obtained from the spin Hamiltonian[4] by expanding the exchange couplings as

$$J^{\alpha\beta}_{ij} = \bar{J}^{\alpha\beta}_{ij} + \frac{\partial J^{\alpha\beta}_{ij}}{\partial \boldsymbol{\varepsilon}_{ij}} \cdot \boldsymbol{\varepsilon}_{ij} + \frac{1}{2}\boldsymbol{\varepsilon}_{ij} \cdot \frac{\partial^2 J^{\alpha\beta}_{ij}}{\partial \boldsymbol{\varepsilon}_{ij} \partial \boldsymbol{\varepsilon}_{kl}} \cdot \boldsymbol{\varepsilon}_{kl}. \tag{5}$$

This leads to the two terms H^{sl}_{M} and $\tilde{H}^{Q}_{sl}$ in Eq. 3.

Together, they represent the couplings of the lattice vibrations with the dipole and quadrupole components.

Coupling of the pseudospins with an external magnetic field: The coupling of the non-Kramers doublet with an external magnetic field is given by

$$H_{\mathrm{z}} = H_{\mathrm{z}}^{m} + H_{\mathrm{z}}^{Q} + H_{\mathrm{z-el}}. \tag{6}$$

The first term is the usual dipolar coupling

$$H_{\mathrm{z}}^{m} = -g_{\mathrm{eff}} \sum_{i} s_i^z \mathbf{h} \cdot \hat{\mathbf{z}}_{\mathbf{i}} = -2 g_{\mathrm{eff}} \sum_{\boxtimes} \mathbf{h} \cdot \mathbf{m}_T. \tag{7}$$

The dipole moment is Ising-like, and the Lande g-factor is $4/5$ for $Pr_2Zr_2O_7$. The second term is the coupling of the Zeeman field with the transverse components of the pseudospins– the quadrupole moments:

$$H_z^Q = \sum_{\boxtimes} \left(\tilde{\lambda}_E \boldsymbol{\xi}^E \cdot \mathbf{Q}_{\boxtimes}^E + \tilde{\lambda}_T \boldsymbol{\xi}^T \cdot \mathbf{Q}_{\boxtimes}^T \right), \tag{8}$$

where $\boldsymbol{\xi}^E = (\sqrt{3}(h_x^2 - h_y^2), (3h_z^2 - h^2))$ and $\boldsymbol{\xi}^T = (h_y h_z, h_x h_z, h_x h_y)$. The third term represents the magnetostriction effect, which will take the following form when the perturbation that breaks the local CEF symmetry are sufficiently small compared to the CEF gap.

$$H_{\mathrm{z-el}} = -g_{\mathrm{eff}} \sum_{i} s_i^z \left[\sum_{p} \boldsymbol{\Gamma}_{ip}^{xz} \cdot \boldsymbol{\varepsilon}_p \hat{x}_i + \sum_{p} \boldsymbol{\Gamma}_{ip}^{yz} \cdot \boldsymbol{\varepsilon}_p \hat{y}_i \right] \cdot \mathbf{h}. \tag{9}$$

The sum p runs over the irreducible representations of the vibrations $\boldsymbol{\varepsilon}$, and $\boldsymbol{\Gamma}$ represents the complete list of magnetostriction coefficients whose magnitude and sign is material dependent.

2. Low-field magnetoelastic effect renormalises quantum dynamics in $Pr_2Zr_2O_7$

The linear quadrupole-strain coupling can lead to a substantial renormalization of the spin-exchange energy scales in the spin-Hamiltonian H_s (Eq. 2), thereby altering the ground-state properties. For

$J_{zz} > J_{\pm}, J_{\pm\pm}, \lambda_{E(T)}$, the low-energy states belong to the ice manifold, and the effect of $\lambda_{E(T)}$ is suppressed as it leads to the creation of magnetic monopoles. The linear spin-phonon coupling Eq. 4 can generate static Jahn-Teller distortion of the tetrahedra $\langle \varepsilon_{\boxtimes} \rangle \neq 0$ at zero magnetic field, realizing a disorder-mediated QSI in an appropriate parameter regime[5,6]. For the new-generation samples a dynamical Jahn-Teller scenario is more suited. In this case, the dynamical lattice vibrations can be integrated out from Eq. 4 to obtain

$$\delta H = -\left[\frac{\lambda_E^2}{\Delta_E} + \frac{\lambda_T^2}{8\Delta_T}\right] \sum_{\langle ij \rangle} (s_i^+ s_j^- + \text{h.c.}) - \frac{\lambda_T^2}{8\Delta_T} \sum_{\langle ij \rangle} (\gamma_{ij} s_i^+ s_j^+ + \gamma_{ij}^* s_i^- s_j^-), \tag{10}$$

which renormalizes the transverse spin exchange (Eq. 2). This renormalization can lead to enhanced transverse (quantum) exchanges, possibly stabilizing a multipolar QSI.

3. The phase diagram for the dynamical Jahn-Teller scenario

At zero magnetic field, once the phonons are integrated out, the Hamiltonian is given by Eq. 2 where the transverse couplings are renormalised via Eq. 10 due to the linear magneto-distortive coupling as discussed above. This Hamiltonian is well known to give rise to a quantum spin ice at low temperatures in the limit $J_{zz} \gg J_{\pm}, J_{\pm\pm}$ [3,7,8]. In this theory, the three excitations are an emergent gapped magnetic monopole (energy gap $\Delta_m \sim J_{zz}$), a gapped electric charge (energy gap from perturbative calculations, $\Delta_e \sim J_{\pm}^3/J_{zz}^2$) and a gapless emergent photon.

For a classical single tetrahedron in a $[111]$ magnetic field, the transition from the "2-in, 2-out" to the "3-in, 1-out" state can be obtained by comparing the J_{zz} term in Eq. 2 and the Zeeman term in Eq. 7. The critical field so obtained is $h_c = \frac{J_{zz}}{2\sqrt{3}g_{eff}}$. The transition is brought about by the condensation of the magnetic monopoles which is easy to see by writing the Ising interactions in terms of the magnetic monopole change m_A (Table 1). However, no symmetries are broken through the transition.

The above estimates are renormalised by both the transverse exchanges and the spin-lattice coupling. The main effect of the transverse couplings is to induce fluctuations of the Ising moments while the spin-lattice coupling, in addition to renormalising various couplings discussed above, lead to magneto-elastic distortion. While a microscopic calculation requires a full solution of the many-body problem, the well-known symmetry analysis based on soft-spin (accounting for the fluctuations) Landau-Ginzburg theory coupled with the elastic modes, provides a satisfactory description of the underlying mechanisms for the magnetodistortive transition in terms of phenomenological parameters of the long-wavelength theory. This is presented below.

Turning to finite temperature, the quantum spin ice gives way to a thermal cooperative magnet (the classical spin ice) via a crossover.[9] This happens due to the proliferation of the electric charges which, within perturbative regime, takes place at $T \sim \Delta_e/k_B$. Due to the spin-phonon coupling, this energy-scale is enhanced as shown in Eq. 10. The first-order magnetodistortive transition at finite field, on the other hand, is expected to survive within the ice manifold and thus end at a critical end-point at $T \sim J_{zz}$. This leads to the schematic phase diagram as shown in Fig. 1. In the material, the above energy-scales are expected to be further dressed by fluctuations and further smaller interactions, but has a similar structure as given in the experimental phase diagram (See Fig. 1**c** in the main text).

To capture the effects due to transverse fluctuations as well as the spin-lattice coupling in the above phase diagram, we now resort to a Landau-Ginzburg theory whose main features are presented in the following sections.

4. The Landau-Ginzburg (LG) theory of the magnetoelastic coupling

The mean field LG free energy density receives various contributions from the dipole, quadrupole and the elastic parts and is given by

$$\mathcal{F} = \mathcal{F}_m + \mathcal{F}_Q + \mathcal{F}_{mQ} + \mathcal{F}_{elastic} + \mathcal{F}_{\rm sl} + \mathcal{F}_{\rm z} + \mathcal{F}_{\rm str} \tag{11}$$

Dipole free energy : $\mathcal{F}_m$ is the free energy contribution of the dipoles and is given by

$$\begin{aligned}\mathcal{F}_m = &\left[\frac{r_{m_A}}{2} m_A^2 + \frac{u_{m_A}}{4} m_A^4\right] + \left[\frac{r_{m_T}}{2} \mathbf{m}_T \cdot \mathbf{m}_T + \frac{u_{m_T}}{4} \left(\mathbf{m}_T \cdot \mathbf{m}_T\right)^2\right] \\ &+ m_A^2 \left[v_m \left(\mathbf{m}_T \cdot \mathbf{m}_T\right) + \tilde{v}_m \left(m_T^{(1)} m_T^{(2)} + m_T^{(2)} m_T^{(3)} + m_T^{(1)} m_T^{(3)}\right)\right].\end{aligned} \tag{12}$$

We expect $(v_m + \tilde{v}_m) < 0$ for a [111] Zeeman field, which leads to an expectation value in m_T. This renormalizes the mass of m_A downward, namely, the magnetic monopole condensation takes place on entry into the ”three-in, one-out” phase.

Quadrupole free energy: The quadrupole contribution $\mathcal{F}_Q$ is given by

$$\begin{aligned}\mathcal{F}_Q = &\left[\frac{r_{Q_E}}{2} \mathbf{Q}_E \cdot \mathbf{Q}_E + \frac{u_{Q_E}}{2} \left(\mathbf{Q}_E \cdot \mathbf{Q}_E\right)^2 + \frac{v_{Q_E}}{3} \left(Q_{E_1}^3 - 3 Q_{E_1} Q_{E_2}^2\right)\right] \\ &+ \left[\frac{r_{Q_T}}{2} \mathbf{Q}_{T_1} \cdot \mathbf{Q}_{T_1} + \frac{u_{Q_T}}{4} \left(\mathbf{Q}_{T_1} \cdot \mathbf{Q}_{T_1}\right)^2 + \frac{v_{Q_T}}{3} Q_{T_1}^{(1)} Q_{T_1}^{(2)} Q_{T_1}^{(3)}\right] \\ &+ v_Q \left[\frac{Q_E^{(1)}}{\sqrt{3}} \left(2 (Q_T^{(1)})^2 - (Q_T^{(2)})^2 - (Q_T^{(3)})^2\right) + \frac{Q_E^{(2)}}{2} \left((Q_{T_1}^{(2)})^2 - (Q_{T_1}^{(3)})^2\right)\right].\end{aligned} \tag{13}$$

The paramagnetic state is obtained when $r_{Q_E}, r_{Q_T} > 0$, while $r_{Q_E}, r_{Q_T} < 0$ yields an antiferro-quadrupolar ordered state.

Dipole-quadrupole interactions: $\mathcal{F}_{mQ}$ is the coupling between dipoles and quadrupoles

$$\begin{aligned}\mathcal{F}_{mQ} =& m_A^2 \left[s_E \mathbf{Q}_E \cdot \mathbf{Q}_E + s_T \mathbf{Q}_{T_1} \cdot \mathbf{Q}_{T_1} \right] \\ &+ w_E \left[\frac{Q_E^{(1)}}{\sqrt{3}} \left(2(m_T^{(1)})^2 - (m_T^{(2)})^2 - (m_T^{(3)})^2 \right) + \frac{Q_E^{(2)}}{2} \left((m_T^{(2)})^2 - (m_T^{(3)})^2 \right) \right] \\ &+ w_T \left[Q_T^{(1)} \left(m_T^{(2)} m_T^{(3)} \right) + Q_T^{(2)} \left(m_T^{(1)} m_T^{(3)} \right) + Q_T^{(3)} \left(m_T^{(1)} m_T^{(2)} \right) \right]. \end{aligned} \tag{14}$$

The above terms are linear in quadrupole and quadratic in dipole fields. The linear coupling between the pseudospins and the elastic modes is particular to the non-Kramers systems and is hence expected to enhance magnetostriction as a more direct feedback.

Elastic free energy: For elastic modes the harmonic energy is given by

$$\mathcal{F}_{elastic} = \frac{1}{2} \left[c_A \epsilon_A^2 + c_E \boldsymbol{\epsilon}_E^2 + c_T \boldsymbol{\epsilon}_T^2 \right], \tag{15}$$

where c_A, c_E and c_T are elastic moduli of the singlet, doublet and the triplet modes, respectively.

Spin-Lattice coupling: The contribution from the spin-lattice coupling is given by

$$\mathcal{F}_{sl} = \mathcal{F}_{\epsilon Q} + \mathcal{F}_{m\epsilon}, \tag{16}$$

where $\mathcal{F}_{\epsilon Q}$ is the coupling of the strain with the quadrupoles

$$\begin{aligned}
\mathcal{F}_{\epsilon Q} = & \left[\Lambda_E \boldsymbol{\epsilon}_E \cdot \mathbf{Q}_E + \Lambda_T \boldsymbol{\epsilon}_T \cdot \mathbf{Q}_T\right] \\
& + \frac{1}{2}\left[\mu_A \epsilon_A + \tilde{\mu}_A \epsilon_A^2 + \tilde{\mu}_E \boldsymbol{\epsilon}_E^2 + \tilde{\mu}_T \boldsymbol{\epsilon}_T^2\right]\left[p_3 \mathbf{Q}_E \cdot \mathbf{Q}_E + p_4 \mathbf{Q}_T \cdot \mathbf{Q}_T\right] \\
& + \mu_{ET}\left[\frac{\epsilon_E^{(1)}}{\sqrt{3}}\left[2(Q_T^{(1)})^2 - (Q_T^{(2)})^2 - (Q_T^{(3)})^2\right] + \frac{\epsilon_E^{(2)}}{2}\left[(Q_T^{(2)})^2 - (Q_T^{(3)})^2\right]\right] \\
& + \xi_E\left[\epsilon_E^{(1)}\left[(Q_E^{(1)})^2 - (Q_E^{(2)})^2\right] - 2\epsilon_E^{(1)} Q_E^{(1)} Q_E^{(2)}\right] \\
& + \xi_T\left[\epsilon_T^{(1)} Q_T^{(2)} Q_T^{(3)} + \epsilon_T^{(2)} Q_T^{(1)} Q_T^{(3)} + \epsilon_T^{(3)} Q_T^{(1)} Q_T^{(2)}\right] \\
& + p_5\left[\frac{Q_E^{(1)}}{\sqrt{3}}\left(2(\epsilon_T^{(1)})^2 - (\epsilon_T^{(2)})^2 - (\epsilon_T^{(3)})^2\right) + \frac{Q_E^{(2)}}{2}\left((\epsilon_T^{(2)})^2 - (\epsilon_T^{(3)})^2\right)\right] \\
& + p_6\left[Q_T^{(1)}\left(\epsilon_T^{(2)}\epsilon_T^{(3)}\right) + Q_T^{(2)}\left(\epsilon_T^{(1)}\epsilon_T^{(3)}\right) + Q_T^{(3)}\left(\epsilon_T^{(1)}\epsilon_T^{(2)}\right)\right]. \qquad (17)
\end{aligned}$$

Similarly, $\mathcal{F}_{m\epsilon}$ gives the coupling of the strains to the dipoles

$$\begin{aligned}
\mathcal{F}_{m\epsilon} = & \left[\lambda_A^M \epsilon_A + \nu_A^M \epsilon_A^2 + \nu_E^M \boldsymbol{\epsilon}_E \cdot \boldsymbol{\epsilon}_E + \nu_T^M \boldsymbol{\epsilon}_T \cdot \boldsymbol{\epsilon}_T\right]\left[p_1 m_A^2 + p_2 \mathbf{m}_T \cdot \mathbf{m}_T\right] \\
& + \lambda_E^M\left[\frac{\epsilon_{E_1}}{\sqrt{3}}\left(2(m_T^{(1)})^2 - (m_T^{(2)})^2 - (m_T^{(3)})^2\right) + \frac{\epsilon_{E_2}}{2}\left((m_T^{(2)})^2 - (m_T^{(3)})^2\right)\right] \\
& + \Lambda_{T_2}^M\left[\epsilon_{T_2}^{(1)}\left(m_T^{(2)} m_T^{(3)}\right) + \epsilon_{T_2}^{(2)}\left(m_T^{(1)} m_T^{(3)}\right) + \epsilon_{T_2}^{(3)}\left(m_T^{(1)} m_T^{(2)}\right)\right]. \qquad (18)
\end{aligned}$$

Thus, the magnetic ordering generically leads to a volume change for the first term with coupling $\lambda_A^M \neq 0$ and also renormalizes the elastic moduli due to the various quadratic couplings.

Zeeman energy: The Zeeman energy for the [111] magnetic field is given by

$$\mathcal{F}_{\mathrm{z}} = -g\ \mathbf{h} \cdot \mathbf{m}_T + \frac{\tilde{\Lambda}_T h^2}{3}\ \mathbf{Q}_T \cdot \hat{\mathbf{z}}_1. \qquad (19)$$

Magnetostriction effect: The magnetostriction effects are given by

$$\begin{aligned}
\mathcal{F}_{\mathrm{str}} = & -\frac{g}{4}\ \epsilon_A m_T^\alpha \gamma_A^{\alpha\beta} h^\beta - \frac{g}{4}\ m_{A_2} h^\alpha (\boldsymbol{\gamma}_E^\alpha \cdot \boldsymbol{\epsilon}_E) - \frac{g}{4}\ m_T^\alpha (\bar{\boldsymbol{\gamma}}_E^{\alpha\beta} \cdot \boldsymbol{\epsilon}_E) h^\beta \\
& - \frac{g}{4}\ m_A h^\alpha (\boldsymbol{\gamma}_T^\alpha \cdot \boldsymbol{\epsilon}_T) - \frac{g}{4}\ m_{T_{1a}}^\alpha (\bar{\boldsymbol{\gamma}}_T^{\alpha\beta} \cdot \boldsymbol{\epsilon}_T) h^\beta. \qquad (20)
\end{aligned}$$

These terms lead to various inter-couplings between the dipolar field and the strain fields in the presence of an external magnetic field.

5. Length change behavior of a multipolar spin ice

The linear coupling between the elastic and spin degrees of freedom (Eqs. 17 and 18) leads to

$$\epsilon_A \approx -\frac{1}{c_A}\left[\frac{\tilde{d}_A p_4 \tilde{\Lambda}_T^2 h^4}{9 r_{Q_T}^2} + \frac{\Lambda_A^M p_2 g^2 h^2}{r_{m_T}^2} - \frac{g^2 h^2}{4 r_{m_T}} \;\hat{h}^\alpha \gamma_A^{\alpha\beta} \hat{h}^\beta + \tilde{d}_A p_3 \mathbf{Q}_E \cdot \mathbf{Q}_E + \Lambda_A^M p_1 m_{A_2}^2\right] \tag{21}$$

$$\epsilon_E^a \approx -\frac{1}{c_E}\left[-\frac{g^2 h^2}{4 r_{m_T}} \;\hat{h}^\alpha \left(\bar{\gamma}_E^a\right)^{\alpha\beta} \hat{h}^\beta + \Lambda_E Q_E^a - \frac{g}{4}\; m_{A_2} h^\alpha \;\left(\gamma_E^a\right)^\alpha\right] \tag{22}$$

$$\epsilon_T^a \approx -\frac{1}{c_T}\left[\frac{\Lambda_T \tilde{\Lambda}_T h^2}{3\sqrt{3} r_{Q_T}} + \Lambda_{T_2}^M \frac{g^2 h^2}{\sqrt{3} r_{m_T}^2} - \frac{g^2}{4}\; m_{A_2} h^\alpha \left(\gamma_T^a\right)^\alpha\right]. \tag{23}$$

The fractional length change along different directions, $\hat{n}$, are related to these expressions such that

$$\left(\frac{\Delta L}{L_0}\right)_{\hat{n}} = \sum_{ij} \epsilon_{ij} n_i n_j. \tag{24}$$

For the $[111]$ direction this gives

$$\begin{aligned}
\frac{\Delta L}{L_0} =& \frac{1}{3}\left[\epsilon_A + 2(\epsilon_{T_1} + \epsilon_{T_2} + \epsilon_{T_3})\right] \\
=& -\frac{1}{3c_A}\left[\frac{\tilde{d}_A p_4 \tilde{\Lambda}_T^2 h^4}{9 r_{Q_T}^2} + \frac{\Lambda_A^M p_2 g^2 h^2}{r_{m_T}^2} - \frac{g^2 h^2}{4 r_{m_T}} \;\hat{h}^\alpha \gamma_A^{\alpha\beta} \hat{h}^\beta\right] - \frac{2}{3c_T}\left[\frac{\Lambda_T \tilde{\Lambda}_T h^2}{\sqrt{3} r_{Q_T}} + \frac{\Lambda_{T_2}^M 3 g^2 h^2}{\sqrt{3} r_{m_T}^2}\right] \\
& -\frac{1}{3c_A}\left[\tilde{d}_A p_3 \mathbf{Q}_E \cdot \mathbf{Q}_E + \Lambda_A^M p_1 m_{A_2}^2\right] + \frac{2}{3c_T}\left[\frac{g^2}{4}\; m_{A_2} h^\alpha \left(\gamma_T^1 + \gamma_T^2 + \gamma_T^3\right)^\alpha\right].
\end{aligned} \tag{25}$$

Similar expressions are derived for the $[100]$ and $[110]$ directions. Each expression contains two contributions – (1) smooth background change, and (2) sharp change generated by the metamagnetic transition where the pseudospin fields gain expectation values. The second contribution is only present for the [111] field direction; thus we expect a smooth field dependence for other field directions, which agrees with the experimental observations (Fig. 2b). The background contribution for different field directions are given by

$$\begin{aligned}
\left(\frac{\Delta L}{L_0}\right)_{[111],background} &= -A_1 h^2 - A_2 h^4 - \frac{2T_1}{3} h^2, \\
\left(\frac{\Delta L}{L_0}\right)_{[100],background} &= -A_1 h^2 - A_2 h^4 - (E_1 - E_2) h^2, \\
\left(\frac{\Delta L}{L_0}\right)_{[110],background} &= -A_1 h^2 - A_2 h^4 - E_1 h^2 - T_1 h^2.
\end{aligned} \tag{26}$$

The temperature-dependent coupling constants A_1, A_2, E_1, E_2 and T_1 determine the sign of the fractional change. $\Delta L/L_0$ also receives contribution from the abrupt change in both the dipole and the quadrupole fields across the first-order metamagnetic transition, which is provided by the following terms

$$\begin{aligned}
\delta\left(\frac{\Delta L}{L_0}\right)_{[111]} &= -A_4 \Delta_A^2 + 2T_4 h\, \Delta_A, \\
\delta\left(\frac{\Delta L}{L_0}\right)_{[100]} &= -A_4 \Delta_A^2 - (E_4 - \sqrt{3} E_5) h \Delta_A, \\
\delta\left(\frac{\Delta L}{L_0}\right)_{[110]} &= -A_4 \Delta_A^2 - (E_4 - T_4) h \Delta_A,
\end{aligned} \tag{27}$$

where A_4, E_4, E_5 and T_4 are temperature dependent LG coupling constants. For the $[111]$ magnetic field, $\delta\left(\mathbf{Q}_E \cdot \mathbf{Q}_E\right) = \delta Q_E^\alpha = 0$ and the jump in m_A across the transition is given by $\delta m_A = \Delta_A$ to the leading order. This contribution has two effects– (1) produce a jump at the metamagnetic transition, and (2) a linear field dependence above the transition; both contributions are direction dependent.

6. Elastic moduli

The renormalized elastic moduli under a magnetic field are given by

$$\begin{aligned}
\tilde{c}_A &= \left[c_A - \frac{g^2h^2\mathcal{A}^\alpha\mathcal{A}^\alpha}{48r_{m_T}}\right], \\
\tilde{c}_E^{ab} &= \left[\left(c_E - \frac{\Lambda_E^2}{r_{Q_E}}\right)\delta_{ab} - \frac{g^2h^2(\tilde{\mathcal{E}}^a\tilde{\mathcal{E}}^b)}{48\tilde{r}_{m_A}} - \frac{g^2h^2(\mathcal{E}^{a\alpha}\mathcal{E}^{b\alpha})}{48r_{m_T}}\right], \\
\tilde{c}_T^{ab} &= \left[\left(c_T - \frac{\Lambda_T^2}{r_{Q_T}}\right)\delta_{ab} - \frac{g^2h^2(\tilde{\mathcal{T}}^a\tilde{\mathcal{T}}^b)}{48\tilde{r}_{m_A}} - \frac{g^2h^2(\mathcal{T}^{a\alpha}\mathcal{T}^{b\alpha})}{48r_{m_T}}\right].
\end{aligned} \tag{28}$$

where $\mathcal{A}, \mathcal{E}$ and $\mathcal{T}$ are combinations of LG couplings introduced in section 3. The sound velocity, v_s, and elastic constants are related by $c = \rho v_s^2$, where ρ is the mass density. Thus the renormalization of the elastic moduli directly affects the sound velocity, such that

$$\frac{\Delta c}{c} \propto \frac{\delta v}{v} \tag{29}$$

7. Low-field thermal expansion and ultrasound renormalization

Following Eq. 11, we calculate the renormalized elastic moduli and the strain fields as a function of temperature at low fields.

Thermal behaviour of ultrasound: In the paramagnetic state, we can integrate out the pseudospin fields to obtain the following renormalization of the three elastic moduli following Ref. 4

and 10. Explicitly for the doublet mode, we have

$$\begin{aligned}\tilde{c}_E =& c_E - \frac{1}{T}\left[\Lambda_E^2 \langle \mathbf{Q}_E \cdot \mathbf{Q}_E \rangle\right] \\ & - \frac{(\Lambda_E^M)^2}{2T}\left[\frac{1}{3}\langle\Big(2(m_T^{(1)})^2 - (m_T^{(2)})^2 - (m_T^{(3)})^2\Big)^2\rangle + \frac{1}{4}\langle\Big((m_T^{(2)})^2 - (m_T^{(3)})^2\Big)^2\rangle\right] \\ & + d_E\left(p_3\langle \mathbf{Q}_E \cdot \mathbf{Q}_E\rangle + p_4\langle \mathbf{Q}_T \cdot \mathbf{Q}_T\rangle\right) + \Lambda_E^M\left[p_1\langle m_A^2\rangle + p_2\langle \mathbf{m}_T \cdot \mathbf{m}_T\rangle\right]. \end{aligned} \tag{30}$$

We obtain similar expressions for c_A and c_T. Focusing on the the doublet mode, the renormalization is given by

$$\Delta c_E = \Delta c_E^Q + \Delta c_E^M, \tag{31}$$

where

$$\Delta c_E^Q = \left(d_E p_3 - \frac{\Lambda_E^2}{T}\right)\langle \mathbf{Q}_E \cdot \mathbf{Q}_E\rangle + d_E p_4 \langle \mathbf{Q}_T \cdot \mathbf{Q}_T\rangle \sim (aT - b)\chi_Q(T) \tag{32}$$

is the contribution from the quadrupoles and

$$\begin{aligned}\Delta c_E^M =& -\frac{(\Lambda_E^M)^2}{2T}\left[\frac{1}{3}\langle\Big(2(m_T^{(1)})^2 - (m_T^{(2)})^2 - (m_T^{(3)})^2\Big)^2\rangle + \frac{1}{4}\langle\Big((m_T^{(2)})^2 - (m_T^{(3)})^2\Big)^2\rangle\right] \\ & + \Lambda_E^M\left[p_1\langle m_A^2\rangle + p_2\langle \mathbf{m}_T \cdot \mathbf{m}_T\rangle\right] \end{aligned} \tag{33}$$

is the contribution from the dipoles.

Thermal expansion: At zero magnetic field, the analogues of Eqs. 21-23 give

$$\epsilon_A = -\frac{1}{c_A}\left[\mu_A\left(p_3\langle \mathbf{Q}_E \cdot \mathbf{Q}_E\rangle + p_4\langle \mathbf{Q}_T \cdot \mathbf{Q}_T\rangle\right) + \lambda_A^M\left(p_1\langle m_A^2\rangle + p_2\langle \mathbf{m}_T \cdot \mathbf{m}_T\rangle\right)\right] \tag{34}$$

$$\epsilon_E^{(1)} = -\frac{1}{c_E}\left[\Lambda_E\langle Q_E^{(1)}\rangle + \frac{\mu_{ET}}{\sqrt{3}}\left[2\langle(Q_T^{(1)})^2\rangle - \langle(Q_T^{(2)})^2\rangle - \langle(Q_T^{(3)})^2\rangle\right]\right]$$
$$-\frac{1}{c_E}\left[\xi_E\left[\langle(Q_E^{(1)})^2\rangle - \langle(Q_E^{(2)})^2\rangle\right]\right] - \frac{1}{c_E}\left[\frac{\lambda_E^M}{\sqrt{3}}\left(2\langle(m_T^{(1)})^2\rangle - \langle(m_T^{(2)})^2\rangle - \langle(m_T^{(3)})^2\rangle\right)\right] \tag{35}$$

$$\epsilon_E^{(2)} = -\frac{1}{c_E}\left[\Lambda_E\langle Q_E^{(2)}\rangle + \frac{\mu_{ET}}{2}\left[\langle(Q_T^{(2)})^2\rangle - \langle(Q_T^{(3)})^2\rangle\right] + 2\xi_E\langle Q_E^{(1)}Q_E^{(2)}\rangle\right]$$
$$-\frac{1}{c_E}\left[\frac{\lambda_E^M}{2}\left[\langle(m_T^{(2)})^2\rangle - \langle(m_T^{(3)})^2\rangle\right]\right] \tag{36}$$

$$\boldsymbol{\epsilon}_T^{(1)} = -\frac{1}{c_T}\left[\Lambda_T\langle Q_T^{(1)}\rangle + \xi_T\langle Q_T^{(2)}Q_T^{(3)}\rangle + \Lambda_T^M\langle m_T^{(2)}m_T^{(3)}\rangle\right] \tag{37}$$
$$\boldsymbol{\epsilon}_T^{(2)} = -\frac{1}{c_T}\left[\Lambda_T\langle Q_T^{(2)}\rangle + \xi_T\langle Q_T^{(1)}Q_T^{(3)}\rangle + \Lambda_T^M\langle m_T^{(1)}m_T^{(3)}\rangle\right] \tag{38}$$
$$\boldsymbol{\epsilon}_T^{(3)} = -\frac{1}{c_T}\left[\Lambda_T\langle Q_T^{(3)}\rangle + \xi_T\langle Q_T^{(1)}Q_T^{(2)}\rangle + \Lambda_T^M\langle m_T^{(1)}m_T^{(2)}\rangle\right] \tag{39}$$

In the paramagnetic phase, we can neglect the linear terms in Q_α to get the following expression for the [111] direction,

$$\left[\frac{\Delta L}{L_0}\right]_{[111]} = \left[\epsilon_A + 2(\epsilon_{T_1} + \epsilon_{T_2} + \epsilon_{T_3})\right]/3 \tag{40}$$
$$= -\frac{1}{3c_A}\left[\mu_A\left(p_3\langle\mathbf{Q}_E\cdot\mathbf{Q}_E\rangle + p_4\langle\mathbf{Q}_T\cdot\mathbf{Q}_T\rangle\right) + \lambda_A^M\left(p_1\langle m_A^2\rangle + p_2\langle\mathbf{m}_T\cdot\mathbf{m}_T\rangle\right)\right]$$
$$-\frac{2}{3c_T}\left[\xi_T\left[\langle Q_T^{(2)}Q_T^{(3)}\rangle + \langle Q_T^{(1)}Q_T^{(3)}\rangle + \langle Q_T^{(1)}Q_T^{(2)}\rangle\right]\right]$$
$$-\frac{2}{3c_T}\left[\Lambda_T^M\left[\langle m_T^{(2)}m_T^{(3)}\rangle + \langle m_T^{(1)}m_T^{(3)}\rangle + \langle m_T^{(1)}m_T^{(2)}\rangle\right]\right] \tag{41}$$

Similar expressions can be obtained for other directions. The form of $\Delta L/L_0$ has qualitative similarities with the ultrasound response– albeit with a different combination of LG couplings. The close resemblance of the experimental data in Figs. 4c and 4d bears out this theoretical expectation.

1. Kimura, K. *et al.* Quantum fluctuations in spin-ice-like $Pr_2Zr_2O_7$. *Nat. Commun.* **4**, 1934 (2013). URL `https://doi.org/10.1038/ncomms2914`.

2. Petit, S. *et al.* Antiferroquadrupolar correlations in the quantum spin ice candidate $Pr_2Zr_2O_7$. *Phys. Rev. B* **94**, 165153 (2016). URL `https://link.aps.org/doi/10.1103/PhysRevB.94.165153`.

3. Lee, S., Onoda, S. & Balents, L. Generic quantum spin ice. *Phys. Rev. B* **86**, 104412 (2012). URL `https://link.aps.org/doi/10.1103/PhysRevB.86.104412`.

4. Bhattacharjee, S. *et al.* Interplay of spin and lattice degrees of freedom in the frustrated antiferromagnet $CdCr_2O_4$: High-field and temperature-induced anomalies of the elastic constants. *Phys. Rev. B* **83**, 184421 (2011). URL `https://link.aps.org/doi/10.1103/PhysRevB.83.184421`.

5. Savary, L. & Balents, L. Disorder-induced quantum spin liquid in spin ice pyrochlores. *Phys. Rev. Lett.* **118**, 087203 (2017). URL `https://link.aps.org/doi/10.1103/PhysRevLett.118.087203`.

6. Martin, N. *et al.* Disorder and quantum spin ice. *Phys. Rev. X* **7**, 041028 (2017). URL `https://link.aps.org/doi/10.1103/PhysRevX.7.041028`.

7. Castelnovo, C., Moessner, R. & Sondhi, S. Spin ice, fractionalization, and topological order. *Annual Review of Condensed Matter Physics* **3**, 35–55 (2012). URL `https://doi.org/10.1146/annurev-conmatphys-020911-125058`.

8. Gingras, M. J. P. & McClarty, P. A. Quantum spin ice: a search for gapless quantum spin liquids in pyrochlore magnets. *Rep. Prog. Phys.* **77**, 056501 (2014). URL `https://doi.org/10.1088/0034-4885/77/5/056501`.

9. Banks, T. & Rabinovici, E. Finite-temperature behavior of the lattice abelian Higgs model. *Nuclear Physics B* **160**, 349–379 (1979). URL `https://doi.org/10.1016/0550-3213(79)90064-6`.

10. Bhattacharjee, S. *et al.* Acoustic signatures of the phases and phase transitions in $Yb_2Ti_2O_7$. *Phys. Rev. B* **93**, 144412 (2016). URL `https://link.aps.org/doi/10.1103/PhysRevB.93.144412`.

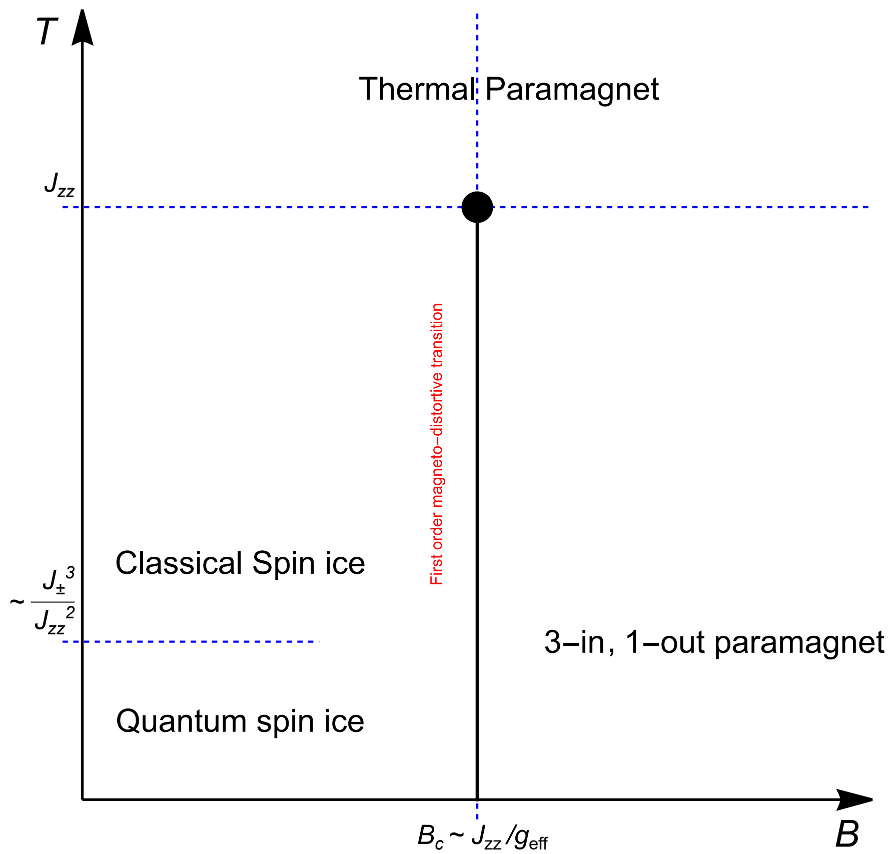

Figure 1: Schematic theoretical phase diagram. The blue dashed lines denote crossovers while the black line denotes the first-order transition ending at a critical end-point.

Table 1: Linear irreducible representations of the spins of a single up tetrahedron.

	Expression in terms of the spins
Dipole Singlet	
m_A	$(s_1^z + s_2^z + s_3^z + s_4^z)/2$
Dipole triplet	
$m_T^{(1)}$	$(s_1^z + s_2^z - s_3^z - s_4^z)/2\sqrt{3}$
$m_T^{(2)}$	$(s_1^z - s_2^z + s_3^z - s_4^z)/2\sqrt{3}$
$m_T^{(3)}$	$(s_1^z - s_2^z - s_3^z + s_4^z)/2\sqrt{3}$
Quadrupole doublet	
$Q_E^{(1)}$	$(s_1^x + s_2^x + s_3^x + s_4^x)/2$
$Q_E^{(2)}$	$(s_1^y + s_2^y + s_3^y + s_4^y)/2$
Quadrupole Triplet-1	
$Q_{T_1}^{(1)}$	$\sqrt{3/2}(-s_1^x - s_2^x + s_3^x + s_4^x)$
$Q_{T_1}^{(2)}$	$(\sqrt{3}s_1^x - 3s_1^y - \sqrt{3}s_2^x + 3s_2^y + \sqrt{3}s_3^x - 3s_3^y - \sqrt{3}s_4^x + 3s_4^y)/6\sqrt{2}$
$Q_{T_1}^{(3)}$	$(\sqrt{3}s_1^x + 3s_1^y - \sqrt{3}s_2^x - 3s_2^y - \sqrt{3}s_3^x - 3s_3^y + \sqrt{3}s_4^x + 3s_4^y)/6\sqrt{2}$
Quadrupole Triplet-2	
$Q_{T_2}^{(1)}$	$(-s_1^y - s_2^y + s_3^y + s_4^y)/2$
$Q_{T_2}^{(2)}$	$\left(\sqrt{3}s_1^x + s_1^y - \sqrt{3}s_2^x - s_2^y + \sqrt{3}s_3^x + s_3^y - \sqrt{3}s_4^x - s_4^y\right)/4$
$Q_{T_2}^{(3)}$	$\left(-\sqrt{3}s_1^x + s_1^y + \sqrt{3}s_2^x - s_2^y + \sqrt{3}s_3^x - s_3^y - \sqrt{3}s_4^x + s_4^y\right)/4$